Polymer−Clay Nanocomposite Latex Particles by Inverse Pickering Emulsion Polymerization Stabilized with Hydrophobic Montmorillonite Platelets

D. J. Voorn,[†,‡] W. Ming,[*,‡] and A. M. van Herk[*,†]

Laboratory of Polymer Chemistry, Eindhoven University of Technology, P.O. Box 513, 5600 MB Eindhoven, The Netherlands, and Laboratory of Materials and Interface Chemistry, Eindhoven University of Technology, P.O. Box 513, 5600 MB Eindhoven, The Netherlands

Received November 28, 2005; Revised Manuscript Received January 24, 2006

ABSTRACT: We present the first surfactant-free inverse emulsion polymerization by using organically modified clay platelets as stabilizers. Colloidally stable inverse Pickering emulsions of aqueous acrylamide (AAm) or 2-hydroxyethyl methacrylate (HEMA) in cyclohexane stabilized by hydrophobic Cloisite 20A (MMT20) were prepared. With both oil-soluble 2,2′-azobis(isobutyronitrile) (AIBN) and water-soluble 2,2′-azobis[2-methyl-*N*-(2-hydroxyethyl)propionamide] (VA-086) as initiators, inverse latexes in the size range of 700−980 nm were successfully obtained. It has been revealed by SEM and cryo-TEM that the latexes were stabilized by hydrophobic clays, as exemplified by the rugged surface of the particles. It was shown from thermogravimetric analysis (TGA) that all the clay platelets were incorporated into the composite particles, and in partially exfoliated state as indicated by X-ray diffraction study.

Introduction

Formation of a stable emulsion from two immiscible liquids in the micrometer or submicrometer range can normally only be obtained by the addition of surface active compounds, like surfactants. Organic latex particles are known to stabilize emulsions and suspensions by assembly at the liquid−liquid interface. Moreover, inorganic particles such as CdSe nanoparticles have also been used to stabilize emulsions.[1] When particles instead of surfactant molecules are used to stabilize the emulsion, the term "Pickering emulsion" is commonly used.[2,3] By reducing the dimensions of the stabilizing particles to the nanoscale, it is possible to generate emulsion droplet sizes down to 50 nm.[4]

Nanoparticles such as layered silicates have a thickness of 1 nm and a width in the submicrometer to micrometer range for the naturally occurring bentonites. These plateletlike particles have been extensively studied in the past years as filler materials for the formation of polymer−clay nanocomposites, combining beneficial properties of both materials, including low density, flexibility, good moldability, high strength, heat stability, and chemical resistance.[5−8] Several attempts have been made to use these layered silicates for in situ formation of nanocomposites by surfactant-stabilized emulsion polymerization.[9−16] Even a polystyrene-encapsulated Laponite composite system has been claimed by Sun et al.[14] via miniemulsion polymerization. Nevertheless, no direct proof of the encapsulation was presented. For emulsion polymerizations in the presence of clay platelets so-called armored latex were commonly synthesized. In a recent publication by Bon et al.[4] stable styrene oil-in-water (O/W) emulsions were prepared by using synthetic hectorites as stabilizer in the absence of surfactants. After the polymerization of styrene a Pickering dispersion of latex particles stabilized by synthetic clay platelets was obtained.

* Corresponding authors. E-mail: (W.M.) w.ming@tue.nl; (A.M.v.H) a.m.vherk@tue.nl.

† Laboratory of Polymer Chemistry, Eindhoven University of Technology.

‡ Laboratory of Materials and Interface Chemistry, Eindhoven University of Technology.

To date, surfactant molecules are usually added to an inverse emulsion polymerization recipe to provide the system with colloidal stability. Nonionic surfactants like Span 80 or anionic surfactants such as AOT (sodium bis-2-ethylhexylsulfosuccinate) are among the most commonly used in inverse emulsion polymerization.[17,18] An essential problem in the preparation of monomer-containing inverse emulsion is its stability before and during the polymerization of the monomer. Attempts have been reported on the optimization of the process of inverse emulsion formation at higher monomer contents and at lower emulsifier concentrations.[19−21] However, unlike direct O/W emulsions the formation of surfactant-free inverse monomer emulsions has not been reported, let alone the so-called surfactant-free inverse emulsion polymerization. Layered silicates have recently been reported in several patents as stabilizers for water-in-oil (W/O) emulsions for cosmetics, drilling liquids and asphalt coatings.[22,23] Binks et al.[24] prepared an inverse emulsion stabilized by hydrophobically modified bentonite particles. Nonetheless, to the best of our knowledge, nanocomposite particles originating from inverse emulsion polymerizations in the presence layered silicates have not been reported. In the following we describe the preparation of polymer/clay composite particles by surfactant-free inverse Pickering emulsion polymerization. The nanocomposite latex particles were characterized by dynamic light scattering, electron microscopy, X-ray diffraction, and thermogravimetric analysis.

Experimental Section

Materials. Cyclohexane (99.9+%, Aldrich) was used as the continuous phase for inverse emulsions without purification. The monomer acrylamide (AAm, 97%, Aldrich) was purified by recrystallization from acetone (Biosolve), 2-hydroxyethyl methacrylate (HEMA, 97%, Aldrich), and methacrylamidopropyl trimethylammonium chloride (MAPTAC, 85% solution, Degussa) were used as received. Inhibitor was removed from the cross-linker *N*,*N*′-methylenediacrylamide (NDA, 98%, Merck) by distillation under reduced pressure of argon. The initiators 2,2′-azobis[2-methyl-*N*-(2-hydroxyethyl)propionamide] (VA-086, 99%,Wako), ammonium persulfate (APS, 99+%, Aldrich), and 2,2′-azobis(isobutyro-

10.1021/ma052539t CCC: $33.50
Published on Web 02/23/2006

Table 1. Experimental Recipes for Polymerizations with and without Hydrophobic Clay Platelets[e]

entry	clay [wt %][d]	surfactant	monomer type	monomer wt %	water [wt %]	cyclohexane [wt %]	cross-linker [wt %]
C304			AAm	4.2	4.7	91.1	0
C284[a]		span 80	AAm	3.9	4.0	92.1	0
C280[a]		span 80	AAm	4.1	4.1	91.7	0.1
C281[b]		AOT	AAm	4.0	4.0	91.9	0.1
C313	0.51		AAm	3.8	4.1	91.6	0
C303	1.42		AAm	2.4	2.6	93.6	0
C300	0.18		AAm	4.2	4.4	91.1	0.1
C306	0.27		AAm	4.0	4.1	91.5	0.1
C305	0.49		AAm	4.1	4.5	90.8	0.1
C298	0.69		AAm	4.2	4.6	90.4	0.1
C312[c]	0.69		AAm	4.2	4.2	90.8	0.1
C314	0.65		HEMA	3.1	3.1	93.2	0
C294	0.47		MAPTAC	4.0	4.0	91.4	0.1

[a] Stabilized by Span 80 nonionic surfactant (surfactant-to-monomer weight ratio of 1:2). [b] Stabilized by AOT surfactant (surfactant-to-monomer weight ratio of 1:2). [c] 0.1 wt % of oil-soluble AIBN as initiator instead of VA-086. [d] Containing the amount of the organic modifying agent. [e] The initiator (VA-086) content was 0.1 wt % for all the polymerizations unless otherwise indicated.

nitrile) (AIBN, 99+%, Aldrich) were used after recrystallization. The surfactants sorbitan mono-oleate (Span 80, Fluka) and sodium bis(2-ethylhexyl) sulfosuccinate (AOT, Aldrich) were used without purification. The layered silicate Cloisite 20A, a dimethyl−ditallow−ammonium organically modified montmorillonite (MMT20), was obtained from Southern Clay Products Inc. The nascent Cloisite 20A particle size distribution was narrowed before addition to the recipe by dispersing the clay in cyclohexane (0.2 wt %) and ultrasonicating for 5 min, followed by centrifugation at 3000 rpm for 30 min using a Mistral 3000E instrument. The supernatant was collected and dried under vacuum for 5 h. This procedure was repeated two more times. Demineralized water was prepared using a Millipore Super Q apparatus.

Inverse Emulsion Polymerization Procedure. Inverse emulsion polymerizations were performed in 100 mL three-neck round-bottom flasks. The reactor was equipped with an argon inlet, a reflux condenser with an outlet to a bubble counter, a thermometer, and a septum through which the samples were withdrawn during the reaction. A typical polymerization procedure is described as follows (entry C298, Table 1). The inverse emulsion was prepared by mixing a solution of AAm, VA-086, and NDA in water to a dispersion of MMT20 in cyclohexane at room temperature. The emulsions were prepared by applying ultrasound for 5 min with a Vibracell VC750 Sonifier while the reactor was continuously cooled with an ice bath to prevent the increase of the dispersion temperature as a result of the ultrasonification. The power to prepare the emulsions was set at 40% for the 3 mm tip and the frequency was fixed at 20 ± 0.2 kHz. After emulsification, the dispersion was flushed with argon for 30 min while the temperature was increased to 50 °C. The reaction temperature during the polymerization was kept constant at 50 °C. At regular time intervals, samples were taken for gravimetric conversion measurements and particle size analysis. Normally, the reaction was completed very quickly, however, to ensure full conversion of the monomer, the reaction mixture was stirred at 50 °C for 3 h. After polymerizations the nanocomposite dispersions were centrifuged at 3000 rpm for 1 h using a Mistral 3000E instrument to remove free clay platelets possibly present in the dispersions, and the particles were then redispersed in cyclohexane. The procedure was repeated once more.

Characterization. A Malvern Zetasizer Nano ZS with a universal dip cell in a glass cuvette was used for the determination of the ζ-potential of the dispersion.

Thermogravimetric analysis (TGA) was performed with a Perkin-Elmer Pyris 6 apparatus under nitrogen at a flow rate of 25 cm^3 min^{-1}. Before TGA, the samples were vacuum-dried for 24 h at 60 °C and then purged by nitrogen. A scanning rate of 10 °C min^{-1} was used.

Scanning electron microscopy (SEM) micrographs were taken using a JEOL JSM-5600 with an acceleration voltage of 15 kV. Polymer−clay composite latex particles were gold-coated prior to scanning. A JEOL 2000 FX transmission electron microscope was used for the particle morphology and size analyses. Latex samples of 0.05 wt % were air-dried on a 400-mesh copper grid with a Formvar supported film.

A Philips TEM CM12 transmission electron microscope was used for the cryo-TEM analysis of the nanocomposite latex samples taken directly after the polymerization was completed. Carbon-coated lacy substrates supported by a TEM 300 mesh copper grids (Quantifoil R2/2) were first cleaned from residual polymer with several cycles of chloroform after which 3 μL of the nanocomposite particle dispersion was placed on the grid. The excess sample was blotted with filter paper, and the resulting thin film was vitrified in liquid ethane at its melting temperature using a Vitrobot vitrification robot.

Number-average diameter ($\overline{D_n}$) and standard deviation (δ) were determined by measuring the diameter of the particles from the SEM and TEM photographs as follows:

$$\overline{D_n} = \frac{\sum_{i=1}^{n} D_i}{n}; \quad \delta = \sqrt{\frac{\sum_{i=1}^{n} (D_i - \overline{D_n})^2}{n-1}}$$

(n is the number of particles counted for calculation, usually 100−200).

The average particle size and particle size distribution of the emulsions and latex particles were determined by means of dynamic light scattering (DLS) performed at 21 °C on a Malvern 4700 light scattering instrument equipped with a Malvern Multi-8 7032 correlator at a scattering angle of 90°.

The nanocomposite latex samples were dried under vacuum at 60 °C for 24 h. Samples prepared without cross-linker were able to form a film, whereas the cross-linked samples had a more powdery appearance. The X-ray diffraction (XRD) measurements were carried out with a Rigaku D/Max-B diffractometer, using Cu Kα radiation at 40 kV and 30 mA. The samples were measured with a step of 0.02° (2θ) and a dwell time of 2 s.

Results and Discussion

Inverse Emulsions Stabilized by Hydrophobic Montmorillonite. Inverse or water-in-oil (W/O) emulsions usually require the addition of low HLB (hydrophilic lipophilic balance) surfactants in the recipe to prevent coalescence of the water droplets. Without the presence of any stabilizing agent no stable emulsion was obtained (entry C304, Table 1). It is well established that solid particles with special features will self-assembly at the liquid−liquid interface to reduce the interfacial energy between the two immiscible liquids (see Figure 1). Dispersions of inorganic particles have been used to prevent

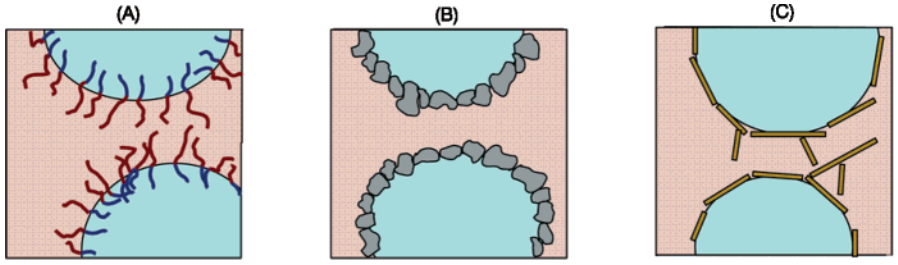

Figure 1. Schematic representation of the stabilization mechanism of inverse emulsions. Key: (a) low HLB surfactants around the water droplets; (b) solid particles around the droplet; (c) an inverse emulsion stabilized by clay platelets where slight bending of the clay is possible, adapted from Lagaly et al.[25]

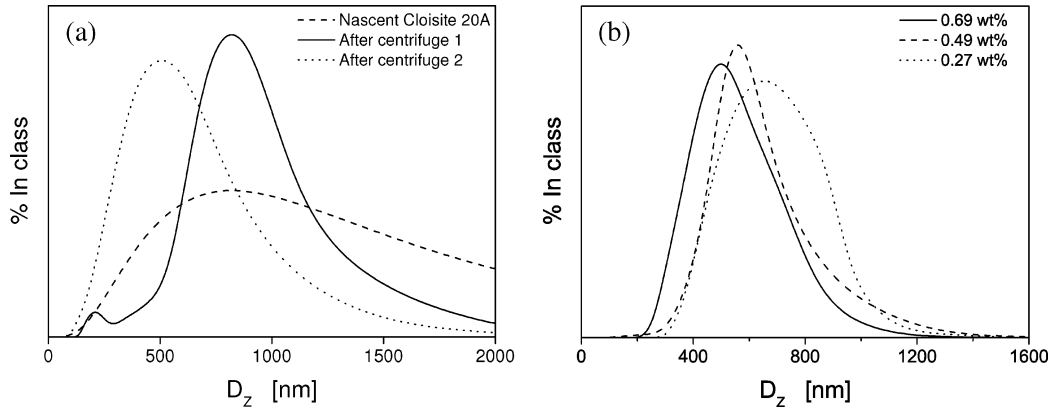

Figure 2. Particle size distribution for (a) Cloisite 20A (MMT20) platelets in cyclohexane before and after centrifugation and (b) for W/O emulsions containing different MMT20 concentrations: 0.27 wt % (C306); 0.49 wt % (C305); 0.69 wt % (C298).

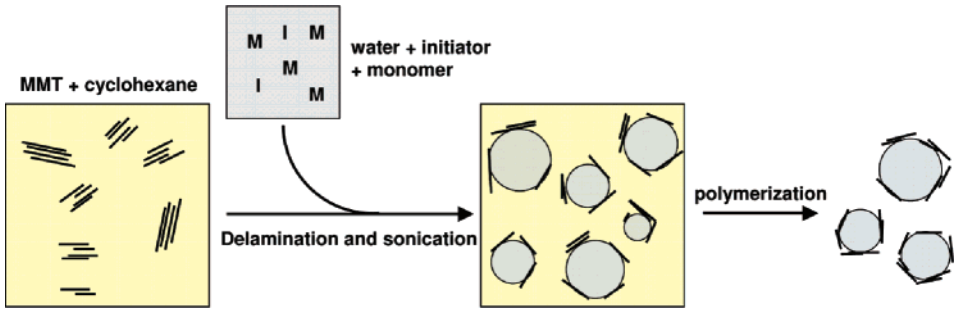

Figure 3. Schematic representation of the inverse emulsion polymerization and the stabilizing function of the hydrophobic clay platelets.

agglomeration.[1] Inorganic clay platelets have been used as stabilizers for emulsions and inverse emulsions.[4,25] For inverse emulsions the sodium ions in naturally occurring clays have been exchanged by organic cations to make the platelets dispersible in the organic medium. The long alkyl chain of the quaternary ammonium compounds that are adsorbed on the surface of the hydrophobized clay surface enables the swelling and exfoliation of the platelets in apolar medium.

Mixing the clay platelets that are dispersed in cyclohexane with the monomer aqueous solution results in a slight increase of the turbidity of the apolar phase. Although the hydrophobically modified clay platelets are dispersed in the organic phase, they tend to adsorb a small portion of water and transport to the cyclohexane phase. This phenomenon was also observed by Binks et al.[24] The increase in turbidity indicates that there are particles formed in the oil phase that scatter light.

Exfoliation and dispersibility of the organically modified clays in cyclohexane was investigated by dynamic light scattering. First the organically modified clay dispersed in cyclohexane showed a broad distribution, most likely due to the association of the clay platelets which form large aggregates (Figure 2a). After an ultrasonication step for 5 min to delaminate the stacked clay platelets and a subsequent centrifugation for 30 min, a significant reduction of the particle size and narrowing of the distribution was observed. A second ultrasonication of the supernatant dispersion followed by another centrifugation step further lowered the average particle size to ∼500 nm (Figure 2a). Additional ultrasonication/centrifuge steps did not reduce the particle size significantly.

For the inverse emulsion polymerizations of acrylamide (AAm) the addition of a small amount of water is needed to dissolve the monomer. In this case a weight fraction of water (ϕ_w) between 2% and 10% is sufficient to dissolve the monomer. Systems with higher ϕ_w values did not produce any stable inverse emulsions in the presence of the MMT20 clay platelets. Inverse emulsions containing around 4 wt % of water and 3.9 wt % of AAm were subsequently prepared by the addition of different amounts of MMT20 platelets and the equivalent spherical diameter of the emulsions was measured after sonication. The average diameter increased with decreasing the concentration of MMT20 from 0.69 to 0.27 wt %, as shown in Figure 2b. On the other hand, when the clay content was too high (1.42 wt %, C303, Table 1), a significant increase of the dispersion viscosity was observed, most likely because of the stacking behavior of the clays in the apolar medium.

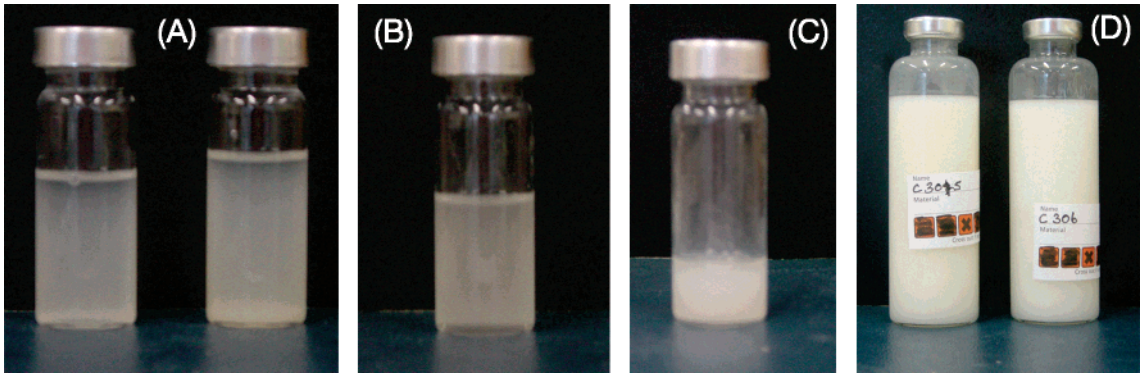

Figure 4. Photographs of inverse AAm emulsions stabilized by hydrophobic clays before and after polymerization: (A) inverse emulsions with 0.27 wt % (C306, left) and 0.49 wt % (C305, right) of clay before sonication; (B) a sample of C305 after 5 min sonication; (C) a sample of C305 after 45 min of polymerization at 50 °C; (D) samples of C305 (left) and C306 (right) after 90 min of polymerization at 50 °C.

Table 2. Total Clay Contents before and after Polymerization and the Average Particle Diameters of Different Starting Emulsions and Final Latexes

	total inorganic content		particle size distribution				
entry	in recipe (wt %)[a]	after polymn (wt %)[b]	D_z [nm][c,d]	PDI	D_z [nm][d,e]	PDI	$\overline{D_n}$ [nm][f]
C300	2.7	2.6	724	0.33	981	0.32	
C306	4.1	3.9	677	0.31	857	0.27	
C305	6.4	6.3	547	0.24	802	0.19	787 ± 57
C298	8.3	8.2	508	0.31	697	0.30	674 ± 69
C312	8.3	8.4	571	0.30	749	0.24	744 ± 52
C314	9.6	9.4	552	0.27	724	0.24	706 ± 48

[a] Total amount of clay in initial recipe based on the monomer content after subtracting the amount of the organic modifier. [b] Determined by TGA analysis of final nanocomposite particles. [c] *Z*-average size for starting inverse emulsions. [d] *Z*-average particle diameter obtained by DLS measurements. [e] *Z*-average size after polymerization. [f] number-average size from SEM and TEM.

The effect of the addition of initiators on the inverse emulsion stability was investigated. When the anionic APS initiator was added to the inverse emulsion, immediate flocculation of the dispersion was observed. Massive flocculation was also observed for the addition of a cationic monomer (MAPTAC) solution to the clay dispersion (C294, Table 1). Apparently, ionic compounds, either anionic or cationic, could induce massive flocculation of the clay platelet dispersions, possibly because of the uncontrolled electrostatic interactions between the anions and the clay edges (positively charged) or the cations and the clay surface (negatively charged). As a consequence, the nonionic water-soluble initiator VA-086 and the oil-soluble AIBN initiator were used, without inducing any flocculation of the dispersion (photos of the stable emulsions are also shown in Figure 4).

We measured the ζ-potential of the clay dispersion in cyclohexane and the inverse emulsions. The organically modified clay platelets dispersed in cyclohexane (after sonication/centrifugation steps) demonstrated a slightly positive ζ potential (0.6 mV). The positive charge likely originates from the edges of the clay platelets, while the surface negative charge on the clay platelets may be shielded by the hydrophobizing agent. On the other hand, no ζ-potentials could be measured for the monomer-containing inverse emulsions stabilized by the clay platelets, which may be the result of a very low concentration of ions in the dispersion. One could speculate about the possibility that the hydrophobizing compounds would be capable of rearranging during the emulsification in order to maximize the hydrophilic surface which is in contact with the water droplets. This rearrangement would make the clay platelet a surfactant-like particle.

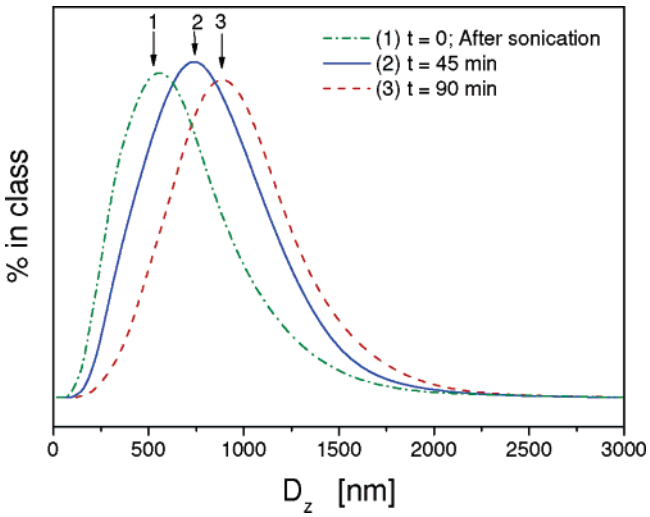

Figure 5. Particle size evolution during the inversion emulsion polymerization stabilized by hydrophobic clays (C305): (1) directly after sonication and after (2) 45 min and (3) 90 min of polymerization at 50 °C.

We attempted to use nascent, unmodified, hydrophilic natural sodium clays as the stabilizer for the inverse emulsions; no stable dispersion was obtained after sonication. We also tried to prepare inverse emulsions using dimethyl-ditallow ammonium chloride (the agent used to hydrophobize the clay) as a surfactant, and it turned out that no stable W/O emulsions could be obtained, either. Only the hydrophobically modified clay platelets appeared to be able to stabilize W/O emulsions without the addition of surfactants. The formed inverse Pickering emulsions can be regarded as surfactant-free inverse emulsions.

Inverse Pickering Emulsion Polymerization. Inverse emulsion polymerizations of acrylamide stabilized by the ionic surfactant AOT (entry C281, Table 1) and the nonionic Span 80 (entry C280) as reference experiments produced latex particles with a final latex particle diameter of around 40 nm, which are comparable with the values reported in the literature.[26] A schematic illustration of the surfactant-free inverse emulsion polymerization in the presence of hydrophobic MMT is given in Figure 3.

Polymerization was started after flushing the system for 15 min with argon and heating to a set point at 50 °C. During the polymerization the color of the dispersion changed from turbid white to more milky white as displayed in Figure 4. After approximately 3 h of polymerization, the reactions were stopped. All the latexes containing nanocomposite particles would sedimentate within several hours for the high concentrations of

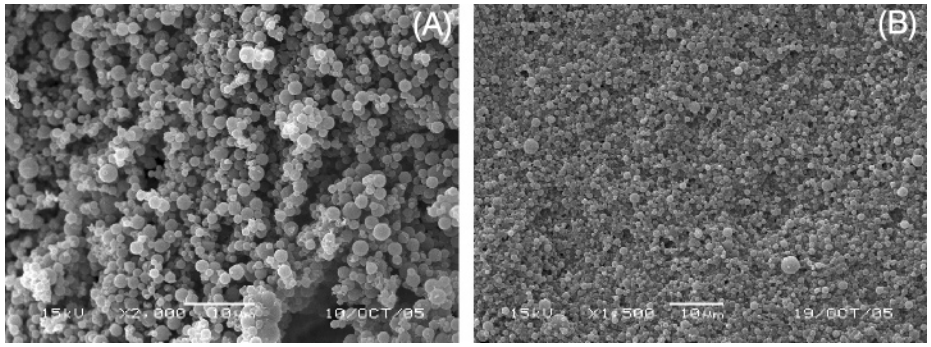

Figure 6. SEM micrographs of PAAm latex particles stabilized by different concentrations of MMT20: (a) C306 with 0.27 wt % clay, and (b) C305 with 0.49 wt % clay (scale bar: 10 μm).

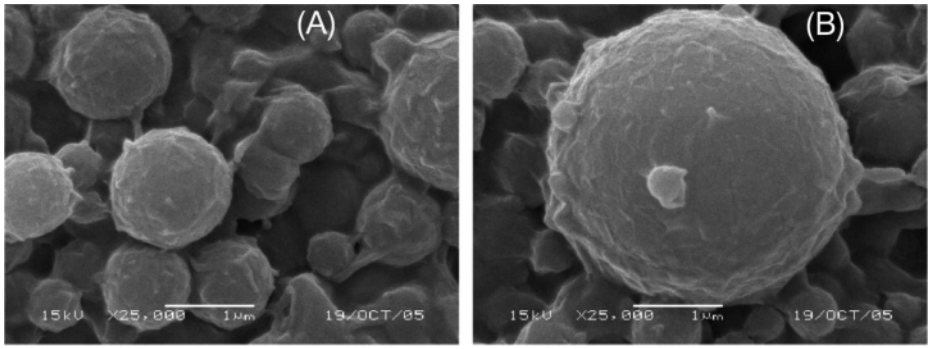

Figure 7. SEM micrographs of PAAm latex particles stabilized by Cloisite 20A clay platelets. Key (a) micrograph of entry C305 with 0.49 wt % of clay platelets; (b) micrograph clearly showing the rugged surface morphology of the PAAm composite particles (scale bar is 1 μm).

clay platelets (C313 and C298) and about 1 day for the systems with lower concentrations (C305 and C306). The sediment could easily be redispersed by shaking the vials or agitation. This sedimentation is expected as a result of the large particle size of the latexes. Table 2 summarizes the initial emulsion droplet sizes before the polymerization and final latex sizes after polymerization. The final particles appeared to be about 200 nm larger than the initial emulsion droplets, while there was no significant change for the PDI. DLS measurements also revealed that the particle size increased gradually during the polymerization. The values for the latexes obtained from DLS are in good agreement with those from electron microscopy analyses. By increasing the concentration of clay platelets in the initial dispersions from 0.18 to 0.69 wt %, a decrease in the particle size (from 980 to 700 nm for the cross-linked latexes was observed (Table 2).

The evolution of the apparent particle size during the inverse emulsion polymerization was monitored by DLS, as shown in Figure 5. As the polymerization proceeded, the particle size increased continuously, indicating that there may be monomer transportation during the polymerization. The particle size increase corresponds to the turbidity change observed in Figure 4 (parts C and D) during the polymerization.

Latex Characteristics. SEM micrographs of final composite latex particles after polymerization for 90 min are depicted in Figure 6. It is clear from these micrographs that by increasing the concentration of MMT20 from 0.27 to 0.49 wt %, the final latex particle size was reduced (see also Table 2). The concentration of clay platelets had a significant influence on the final composite particle size, and by changing the concentration, it was possible to control the final latex particle size. Enlargements of latex particles from sample C305 are shown in Figure 7. It is clearly visible that the clay platelets are located at the surface of the latex particle, similar to what has been reported by Bon et al.[4] The rugged surface morphology in Figure 7b clearly indicates that the PAAm latex particles are covered by a layer of clay platelets.

SEM analysis provides clear morphological information on the particles in the dry state; we also used cryo-TEM to observe the real particle morphology in the liquid state. Although most of the cryo-TEM work has been done on aqueous systems, several investigations using organic solvents have been published.[27,28] Direct vitrification of cyclohexane or toluene by liquid nitrogen produced partial stable glassy films with some crystallization. The cloudy background in TEM micrographs (Figure 8) may be due to the frozen solvent which has partially crystallized. Details on handling inverse emulsion systems for cryo-TEM analysis will be reported elsewhere.[29]

A "fluffy" structure was clearly formed around the particles, as can be seen in Figure 8. On the other hand, the partial exfoliation of the clay platelets in the organic medium was observed, indicating that clay platelets are difficult to completely exfoliate in apolar medium. In some case, bundles of several stacked platelets were found, but the vast majority of these platelets were shown to be located around the latex particles. The hydrophobic clay platelets appeared to be partially "stretched" out into the organic medium. The difference between the SEM and cryo-TEM observations is very likely due to the SEM sample preparation: the "fluffy" clay platelets become collapsed on the surface of the latex during drying.

It has been reported[20,30,31] that the inverse emulsion polymerization mechanism shows analogues to the conventional oil-in-water emulsion polymerization process. It has been shown that the ingredients and the recipe have a significant influence on the kinetics of the polymerization. Although fundamental differences between polymerizations using oil-soluble and water-soluble initiators are known, the composite latex particles depicted in Figure 8 show similar particle morphologies. Apparently not much difference for the latexes prepared with the water-soluble initiator VA-086 (C306) and with the oil-

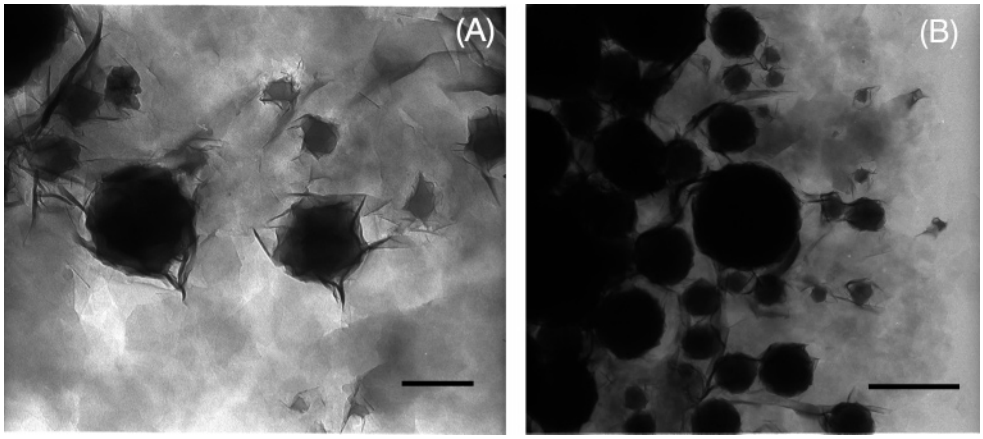

Figure 8. Cryo-TEM micrographs of PAAm latexes prepared with a water-soluble initiator VA-086, entry C306 (a), and an oil-soluble initiator AIBN, entry C312 (b) (scale bar is 1 μm).

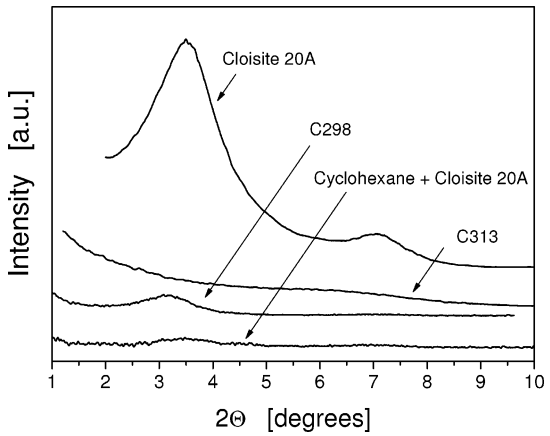

Figure 9. X-ray diffraction patterns of Cloisite 20A after drying, 2 wt % Cloisite 20A dispersed in cyclohexane, un-cross-linked nanocomposite particles (C313), and cross-linked nanocomposite particles (C298).

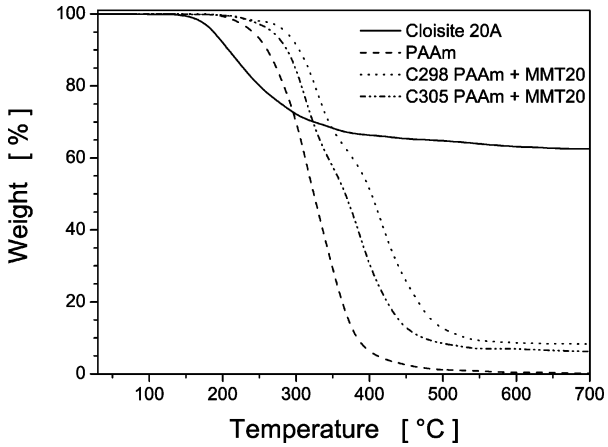

Figure 10. TGA traces for Cloisite 20A, polyacrylamide (PAAm) homopolymer latex (C284), and PAAmclay nanocomposite latexes (C298 and C305).

soluble initiator AIBN (C312) was observed. The morphology observed by TEM indicates that for both initiators the clay platelets are mainly located at the surface of the latex particles.

To check the influences of different monomers on the formation of composite latex particles by inverse emulsion polymerization, another hydrophilic monomer HEMA was used (C314, Table 1). The droplet size of the MMT20-stabilized HEMA inverse emulsion was in the similar size range to the AAm emulsions, as given in Table 2. HEMA could be polymerized to form latex particles of about 720 nm (Table 2); however, the formed latex was less stable than the PAAm latexes. Furthermore, the content of fouling in the reactor formed during the reaction was much higher than the PAAm-based particles.

X-ray diffraction (XRD) was used to study the organization and exfoliation of clay platelets inside a polymer matrix. Figure 9 shows the XRD patterns of the organically modified Cloisite 20A, the Cloisite dispersed in cyclohexane, and nanocomposite latex particles. For the Cloisite 20A, a peak appeared at $2\theta = 3.48°$, corresponding to the basal spacing (d_{001}) of 2.54 nm, and a secondary peak was observed at $2\theta = 7.08°$. In the 2 wt % dispersion of clay in cyclohexane only a very weak peak at $2\theta = 3.48°$ was observed, indicating that the clay platelets may be in a partially exfoliated state in the organic medium. The nanocomposite particles were measured after drying in a vacuum for 24 h at 60 °C. For the cross-linked PAAm nanocomposites (C298) a small peak was observed at around 3.36° (Figure 9). The cross-linking in the PAAm particles prevented the latex particles from film formation during the drying; hence, the orientation could only be obtained via the stacking of neighboring MMT20 sheets on the surface of the latex particles. In the un-cross-linked nanocomposites (C313), which was able to form a film upon drying, the d_{001} peak of the clay completely disappeared and only a very small, broad peak was observed at $2\theta = 6.3°$ corresponding to a *d*-spacing of 1.4 nm (this could be due to the possible surfactant migration during the film formation of the sample), indicating the majority of the clays are in exfoliated states in the film. We also attempted to collect XRD patterns in the 2θ range of $0.1-1°$. There were indications of weak peaks at $2\theta = 0.5-0.6°$ (corresponding to *d*-spacing of 15−20 nm) for the un-cross-linked sample C313, suggesting that there may be long-range ordering in the film. In comparison, a smooth curve for the sample C298 containing cross-linked PAAm in the 2θ range of $0.1-1°$ was observed. More investigations are under way.

TGA was used to determine the total inorganic content present in the nanocomposite latex particles. The weight loss curves as a function of temperature for the organically modified clay, the pure PAAm latex, and the composite latex particles are given in Figure 10. There was about 34 wt % weight loss at 700 °C for Cloisite 20A, which is in agreement with the theoretical presence of 95 mequiv of organic ammonium salt ($M_w = 551.6$ g/mol). The pure PAAm latex particles started to decompose at a temperature around 200 °C and were completely combusted at approximately 500 °C. Entries C298 and C305 are nanocomposite particles with a total clay concentration of 12.4 and

9.5 wt % (with modifying agents), respectively. The nanocomposites showed a delayed decomposition compared to the polymeric sample, even though the delayed decomposition is much less significant compared to conventional polymer−clay nanocomposites prepared by melt intercalation of reactive blending that have a more homogeneous distribution of platelets inside the polymer matrix. The homogeneous distribution of the clays hinders the diffusion of the volatile decomposition materials, which contributes to the increased thermal stability.[32] After heating the nanocomposites to 700 °C and leaving them isothermally for 30 min, 8.2 wt % for C298 and 6.3 wt % for C305 of solid material remained in the chamber. These values are well in accordance with the inorganic content that had been incorporated in the composite particles (8.3 wt % and 6.4 wt % for C298 and C305, respectively, after deducting the amount of the modifying agent; see Table 2). This means that either no free clay or a negligible amount of clay was present in the composite latex dispersions.

Conclusions

We have demonstrated that surfactant-free inverse emulsion polymerizations can be successfully carried out by using organically modified clay platelets as stabilizing particles. The hydrophobic clay platelets were primarily located at the oil/water interface, enabling the formation of the inverse Pickering emulsions and the subsequent polymerization of the hydrophilic monomers. The particle size of the PAAm nanocomposite latexes depended on the clay amount: a size range of 700−980 nm could be tuned with a clay content of up to 0.7 wt % in the dispersions. The rugged surface of the particles from microscopic investigations clearly suggests that the hydrophobic clays are located at the particle surface. This study expands the scope of the formation of polymer−clay nanocomposite by emulsion polymerization.

Acknowledgment. The financial support from the Dutch Polymer Institute (DPI) research program Coatings Technology, Project No. 424 and the Foundation of Emulsion Polymerization (SEP) is greatly appreciated. We thank Henk Woestenberg for SEM analyses, Macro Hendrix for XRD measurements, and Wouter Gerritsen for TGA measurements. Special thanks are extended to Dr. P. M. Frederik and P. H. H. Bomans (University of Maastricht, The Netherlands).

References and Notes

(1) Lin, Y.; Skaff, H.; Emrick, T.; Dinsmore, A. D.; Russell, T. P. *Science* **2003**, *299*, 226−229.
(2) Wamsden, W. *Proc. R. Soc. London* **1903**, *72*, 156−164.
(3) Pickering, S. U. *J. Chem. Soc.* **1907**, *91*, 2001−2021.
(4) Cauvin, S.; Colver, P. J.; Bon, S. A. F. *Macromolecules* **2005**, *38*, 7887−7889.
(5) Usuki, A.; Hasegawa, N.; Kato, M. *Adv. Polym. Sci.* **2005**, *179*, 138−195.
(6) Vaia, R. A.; Price, G.; Ruth, P. N.; Nguyen, H. T.; Lichtenhan, J. *Appl. Clay Sci.* **1999**, *15*, 67−92.
(7) Giannelis, E. P.; Krishnamoorti, R.; Manias, E. *Adv. Polym. Sci.* **1999**, *138*, 109−147.
(8) Alexandre, M.; Dubois, P. *Mater. Sci. Eng.* **2000**, *28*, 1−63.
(9) Lee, D. C.; Jang, L. W. *J. Appl. Polym. Sci.* **1996**, *61*, 1117−1122.
(10) Putlitz, B.; Landfester, K.; Fischer, H.; Antonietti, M. *Adv. Mater.* **2001**, *13*, 500−503.
(11) Huang, X.; Brittain, W. J. *Macromolecules* **2001**, *34*, 3255−3260.
(12) Choi, Y. S.; Wang, K. H.; Xu, M.; Chung, I. J. *Chem. Mater.* **2002**, *14*, 2936−2939.
(13) Li, H.; Yu, Y.; Yang, Y. *Eur. Polym. J.* **2005**, *41*, 2016−2022.
(14) Sun, Q.; Deng, Y.; Wang, Z. L. *Macromol. Mater. Eng.* **2004**, *289*, 288−295.
(15) Qutubuddin, S.; Fu, X.; Tajuddin, Y. *Polym. Bull. (Berlin)* **2002**, *48*, 143−149.
(16) Choi, Y. S.; Choi, M. H.; Wang, K. H.; Kim, S. O.; Kim, Y. K.; Chung, I. J. *Macromolecules* **2001**, *34*, 8978−8985.
(17) Xu, Z. Z.; Wang, C. C.; Yang, W. L.; Deng, Y. H.; Fu, S. K. *J. Magn. Magn. Mater.* **2004**, *277*, 136−143.
(18) Ge, L.; Texter, J. *Polym. Bull. (Berlin)* **2004**, *52*, 297−305.
(19) Candau, F.; Zekhnini, Z.; Durand, J.-P. *J. Colloid Interface Sci.* **1986**, *114*, 398−408.
(20) Candau, F.; Collin, D.; Kern, F. *Makromol. Chem. Macromol. Symp.* **1990**, *31*, 27−40.
(21) Candau, F.; Buchert, P. *Colloids Surf.* **1990**, *48*, 107−122.
(22) Bragg, J. R.; Varadaraj, R. WO 03−057793A1, 2003.
(23) Huber, G.; Keilhofer, G.; Plank, J. U.S. Patent 2005−0113261, 2005.
(24) Binks, B. P.; Clint, J. H.; Whitby, C. P. *Langmuir* **2005**, *21*, 5307−5313.
(25) Lagaly, G.; Reese, M.; Abend, S. *Appl. Clay Sci.* **1999**, *14*, 83−103.
(26) Juranicova, V.; Kawamoto, S.; Fujimoto, K.; Kawaguchi, H.; Barton, J. *Angew. Makromol. Chem.* **1998**, *258*, 27−31.
(27) Butter, K.; Bomans, P. H.; Frederik, P. M.; Vroege, G. J.; Philipse, A. P. *Nat. Mater.* **2003**, *2*, 88−91.
(28) Gu, G.; Zhou, Z.; Xu, Z.; Masliyah, J. H. *Colloids Surf. A* **2003**, *215*, 141−153.
(29) Voorn, D. J.; Ming, W.; Bomans, P. H. H.; Frederik, P. M.; van Herk, A. M., in preparation.
(30) Landfester, K.; Willer, M.; Antonietti, M. *Macromolecules* **2000**, *33*, 2370−2376.
(31) Barton, J.; Stillhammerova, M.; Lezovic, M. *Angew. Makromol. Chem.* **1996**, *273*, 99−112.
(32) Burnside, S. D.; Giannelis, E. P. *Chem. Mater.* **1995**, *7*, 1597−1600.

MA052539T